APPENDIX C

Publications

Publication I

Electronic properties of alkoxy derivatives of poly(para-phenylenevinylene), investigated by time dependent density functional theory calculations.

Suramitr, S., Kerdchareon, T., Srikhirin, T., and Hannongbua, S.

Synth. Met., 2005, 155: 27-34.

Available online at www.sciencedirect.com
SCIENCE DIRECT
Synthetic Metals 155 (2005) 27–34
SYNTHETIC METALS
www.elsevier.com/locate/synmet

Electronic properties of alkoxy derivatives of poly(*para*-phenylenevinylene), investigated by time-dependent density functional theory calculations

Songwut Suramitr[a], Teerakiat Kerdcharoen[b,c], Toemsak Srikhirin[b,c], Supa Hannongbua[a,*]

[a] *Department of Chemistry, Faculty of Science, Kasetsart University, Bangkok 10900, Thailand*
[b] *Department of Physics, Faculty of Science, Mahidol University, Bangkok 10400, Thailand*
[c] *Institute of Science and Technology for Research and Development, Mahidol University, Salaya Campus, Nakorn Pathom 73170, Thailand*

Received 13 October 2004; received in revised form 11 April 2005; accepted 6 May 2005
Available online 12 October 2005

Abstract

Geometries and energy gaps of poly(*para*-phenylenevinylene) oligomers (OPV_N) and their alkoxy derivatives were investigated, based on quantum-chemical calculations. This oligomer series includes poly(*para*-methoxy-PV) (DMO-OPV_N), poly(*para*-hexoxy-PV) (DHO-OPV_N) and poly(2-methoxy,5-(2′-ethyl-hexyloxy)-PV) (MEH-OPV_N). Potential energy hypersurfaces of all OPV_2 and OPV_2-alkoxy derivatives were calculated by the semiempirical AM1 and ab initio method at the HF/3-21G and HF/6-31G levels. The results obtained indicate that OPV_2 provide two conformational structures, one coplanar and one twisted. For its alkoxy derivatives, the stable conformation was found to be that in which the two adjacent phenylene rings were coplanar. An intramolecular weak hydrogen bond interaction was also found to occur between the oxygen atom of the alkoxy derivatives and the hydrogen atom of the vinylene linkage. By using these linear relationships, they can be employed to semiquantitatively estimate the first excitation energy. We introduce the relationships with the working function of $E_{expt} = 0.604E_{TDDFT\text{-}B3LYP/6\text{-}31G} + 0.947$ and $E_{expt} = 0.604E_{TDDFT\text{-}B3LYP/6\text{-}31G^*} + 0.983$, based on the geometry obtained from HF/3-21G for corrected the extrapolated energy gaps of DMO-OPV_N, DHO-OPV_N and MEH-OPV_N. It was found that satisfactory linear relationship and TDDFT method can be used to predict the lowest excitation energies for compounds in these systems and applicable to the design of new conducting polymers.

Keywords: Excitation energy; Quantum-chemical calculations; Conductive polymer; Alkoxy derivatives of poly(*para*-phenylenevinylene)

1. Introduction

The vast interest of polymer scientists towards conjugated organic polymers is mainly due to two important discoveries. In 1977, high conductivity was measured on doped polyacetylene [1]. In 1990, electroluminescence was observed from these polymers and light emitting diodes were developed based on these materials [2,3]. After these discoveries, various conjugated polymers were investigated. Poly(*para*-phenylenevinylene) (PPV) is one of the most important conductive polymers studied worldwide because of the ease of processing and tuning of electronic and optical properties by modifying the polymer side chain. Derivatives of PPV have been synthesized by attaching alkoxy side groups onto the phenylene ring at the carbon atoms 3 and 6 (Fig. 1), leading to an increase of both their solubility and stability. Thus, the unique structures of the PPV derivatives yield an attractive combination of electronic and mechanical properties that represent promising materials from an engineering viewpoint.

There are several experimental [4–6] and theoretical [7–10] studies that investigate physical and chemical properties of PPV and its derivatives. For electronic and optical properties, the transition (or excitation) energy from the

* Corresponding author. Tel.: +66 2 942 8900x217; fax: +66 2 579 3955.
E-mail addresses: g4684002@ku.ac.th (S. Suramitr), sctkc@mahidol.ac.th (T. Kerdcharoen), sctsk@mahidol.ac.th (T. Srikhirin), fscisph@ku.ac.th (S. Hannongbua).

0379-6779/$ – see front matter © 2005 Elsevier B.V. All rights reserved.
doi:10.1016/j.synthmet.2005.05.016

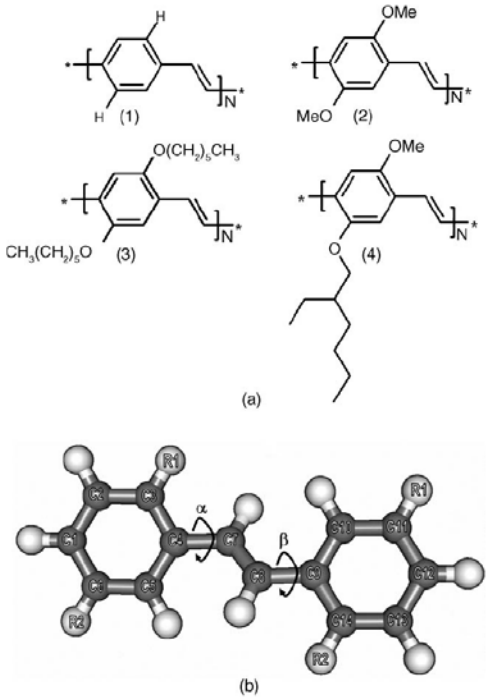

Fig. 1. (a) Illustration of the chemical structure of OPV_N-alkoxy derivatives. Poly(*para*-phenylenevinylene) OPV_N: R1=R2=H; poly(*para*-methoxy)-PV) DMO-OPV_N: R1=R2=O—CH_3 poly(*para*-hexoxy-PV) DHO-OPV_N: R1=R2=O—$(CH_2)_5$—CH_3; poly(2-methoxy,5-(2′-ethyl-hexyloxy)-PV) MEH-OPV_N: R1=OCH_3; R2=O—$CH_2CH(C_2H_5)(C_4H_9)$ and (b) schematic representation of OPV_2 derivatives. α is defined as ∠C3-C4-C7-C8 and β as ∠C7-C8-C9-C14 torsion angle.

ground-state to the first dipole-allowed excited state can be calculated theoretically and used to compare directly with the experimental energy gap. The implicit assumption underlying this approximation is that the lowest singlet excited state can be described by only one singly excited configuration in which an electron is promoted from the Highest Occupied Molecular Orbital (HOMO) to the Lowest Unoccupied Molecular Orbital (LUMO). In fact, the orbital energy difference between HOMO and LUMO is a crude estimation of the transition energy and an accurate description of the lowest singlet excited state requires a linear combination of a number of excited configurations. Despite such deficiency, the calculated HOMO–LUMO gap agrees qualitatively with the experimental energy gap in many cases [11–14]. There exist a variety of theoretical approaches for evaluating this quantity for oligomers as well as infinite polymers. The crudest estimate is the orbital energy difference between the HOMO and LUMO, obtained from Hartree-Fock (HF) or density functional theory (DFT) calculations. Among those theories, Hartree-Fock (HF)-based methods such as configuration interaction singles (CIS) [15] and the random phase approximation (RPA), which is equivalent to the time-dependent HF (TDHF) [16], usually provide only the qualitative or semi-quantitative descriptions for the low-lying excited states. Fortunately, time-dependent density functional theory (TDDFT) [17–20] was a success to some extent. The fusion of a significant quantitative improvement and moderate computational cost has attracted the increasing favor of chemists. Over the past few years, it has advanced to one of the most popular theoretical approaches to calculate excited state properties of medium-sized and large molecules up to about 200 second-row atoms. Moreover, TDDFT method was also successfully employed to extrapolate energy gaps of the polymers from the calculated excitation energies of the oligomers [21–25]. These have pointed out that TDDFT systematically underestimated the excitation energies by 0.4–0.7 eV compared to the experimental results [22–24,26]. The reason for this is due to the limitation of the current approximate exchange-correlation functionals in correctly describing the exchange-correlation potential in the asymptotic region [27]. However, reasonable results can still be expected here because HF/DFT hybrid functionals such as B3LYP can partially overcome the asymptotic problem [23,28]. For linear oligoenes, recent studies on the excited state energies of the first dipole-allowed, ^{1}Bu, states also showed that TDDFT calculations with the B3LYP functional correctly reproduce the general trend of decreasing excitation energy with increasing chain length, with a systematic underestimation of only approximately 0.3–0.5 eV [24–26]. Therefore, TDDFT with the B3LYP functional is expected to be a relatively reliable tool for evaluating the excitation energies of the low-lying excited states for small- and medium-sized molecules.

Recently, extremely ordered crystalline films of some oligomeric materials have been achieved [29–32] for PPV molecule, opening the way to the comparison with accurate theoretical studies by HF and DFT methods. The obtained results indicate that interchain interactions are very sensitive to the structure, and can thus be used to tailor the transport properties of conjugated-polymer films. Consequently, these can be performed by using the solid-state physics implementations that provide reliable microscopic information on structural and electronic properties of extended systems [31,33]. However, Zheng et al. [33] had shown that the calculated electronic properties of PPV isolated chain agree well with the other available theoretical data more than the crystalline state as the interchain effects play a significant role to HOMO and LUMO energy for oligomeric system. Taken into account, in this present work, we focus on excitation energy calculations of the PPV isolate oligomers by using TDDFT methods.

In addition, the effects of substituent size and molecular symmetry on the geometry and excitation energy of alkoxy derivatives of OPV_N were investigated by quantum-chemical calculations. The so-called "oligomer approach" [34] can be used to model the single chain properties of the full polymer.

For examples, HOMO–LUMO energy gaps of the polymers are estimated by extrapolating the excitation energies of the oligomers to infinite chain length. Although the model system is far simpler than the real polymer, it has successfully provided understanding of the experimental results. Energy gaps for poly(*para*-phenylenevinylene) and its derivatives are reproduced to within 0.1 eV of the experimental values without shifting or scaling and provided better results than previous studies [26]. The influence of intrachain ring torsional angles and interchain interactions on the energy gap is also investigated for OPV_N derivatives. Understanding of these factors will lead to more systematic tailoring of energy gaps and improve conductive polymers for electronic devices.

2. Methods of calculation

Starting geometries of the oligomers were constructed using the SciPolymer 3.0 program [35]. The OPV_N derivatives were modified by attaching alkoxy groups onto the phenylene ring at the C3 and C6 atoms. In this work, the notation OPV_N represents the oligomers of PPV with N corresponding to the total number of phenylene rings in the oligomers. The oligomers of OPV_N derivatives are denoted by DMO-OPV_N, DHO-OPV_N and MEH-OPV_N. Their chemical structures are illustrated in Fig. 1(a).

The potential energy surface of each polymer, OPV_2, DMO-OPV_2, DHO-OPV_2 and MEH-OPV_2, was investigated by partial optimization, based on the semiempirical AM1 method [36] and an ab initio calculation at the HF/3-21G and HF/6-31G levels. All calculations were implemented in Gaussian98 [37], running on a Linux PC 2.4 MHz. As these polymers show flexibility in the molecule, potential energy hypersurfaces around the α torsion angle (∠C3-C4-C7-C8) and β torsion angle (∠C7-C8-C9-C14) were also calculated (Fig. 1(b)).

The ground-state geometries of the oligomers were fully optimized using the Hartree-Fock method (HF/3-21G). The chains were found to have coplanar conformations. The calculations of the excitation energies were then performed based on the ground-state geometries. Excitation energies were calculated using the TDDFT (B3LYP/6-31G) and TDDFT(B3LYP/6-31G*) methods and extrapolated to the polymer. We focused on the first excited state with significant oscillator strength (a π–π^* transition), which was also the lowest excited state for all oligomers.

3. Results and discussion

3.1. Conformational analysis of OPV_2 derivatives

The potential energy surface (PES) of unsubstituted OPV_2 based on the AM1, HF/3-21G and HF/6-31G methods are shown in Fig. 2. Based on PES, two minima around the planar conformations (0 and 180°) were observed. It is interesting to note that the oligomer prefers 15–30° off-planar conformations, with the energy difference of less than 0.3 kcal/mol. In particular on OPV_2 system, there are quite flat potential energy curves found at two minima. Elastic neutron-scattering diffraction measurements [38] on oriented OPV_N demonstrated that the phenylene rings were rotated relative to the vinylene linkages by about $7 \pm 6°$ from the planarity. Fig. 2(a) demonstrates that the potential energy of OPV_2 around the minima is rather flat. The rotational barriers are quite small and amount to 1.5, 2.4 and 3.5 kcal/mol with AM1, HF/3-21G and HF/6-31G, respectively. All methods predict that the two phenylene rings are twisted by about 15–30° for both α and β torsion angles in the most stable conformation.

The results of the alkoxy derivatives DMO-OPV_2, DHO-OPV_2 and MEH-OPV_2, (Fig. 2(b–d)) are similar to that of OPV_2 as there are two pronounced minima observed. However, for all three OPV_2 derivatives, it appears that the conformations with a torsional angle close to 180° are more stable than the twisted ones. An explanation for that might be that the OPV_2 derivatives are attributed by the weak hydrogen bonding between the oxygen atom in the methoxy group and the hydrogen atom in the vinylene unit as shown in Fig. 3. The distance of the weak hydrogen bonding was reported to be 2.40 ± 0.40 Å [39].

3.2. Geometries

The optimized geometrical parameters for the phenyl-capped tetramers (hereafter denoted by $N = 4$ since it contains four phenyl rings) of OPV_N and derivatives are summarized in Table 1. For the sake of simplicity, the averages of the bond-length values are reported. Considering the *trans*-stilbene molecule (OPV_2), we found good agreement between the HF/3-21G optimized bond-lengths and the X-ray diffraction study [40]. In Table 1, we also considered the distance between the hydrogen atoms at the vinylene linkage attached on C7 (H′) and C8 (H″) and the hydrogen atoms attached on C3 (H1) and C14 (H2). The distance R(H′–H1) equals to R(H″–H2), $R = 2.37$ Å. Investigation of the torsion angle ∠C3-C4-C7-C8 and ∠C7-C8-C9-C10 indicates that in the geometries of alkoxy OPV_N both phenylene rings are oppositely twisted within the range of 20.1–20.6° out of the planarity. This observation is also supported by the report of Mao [38] and Traetterg [40] who found similar results for stilbene.

The optimized AM1 and HF/3-21G bond distances R(H–O) and bond angles for OPV_N derivatives are presented in Table 1. In this table, the calculated structural parameters indicate intramolecular interactions between the oxygen atom of the substituents and the hydrogen atom of the vinylene linkage. The distances R(H′–O1) and R(H″–O2) obtained from AM1 (R(H–O) = 2.34 Å) are larger than from HF/3-21G (R(H–O) = 2.24 Å). These results suggest that

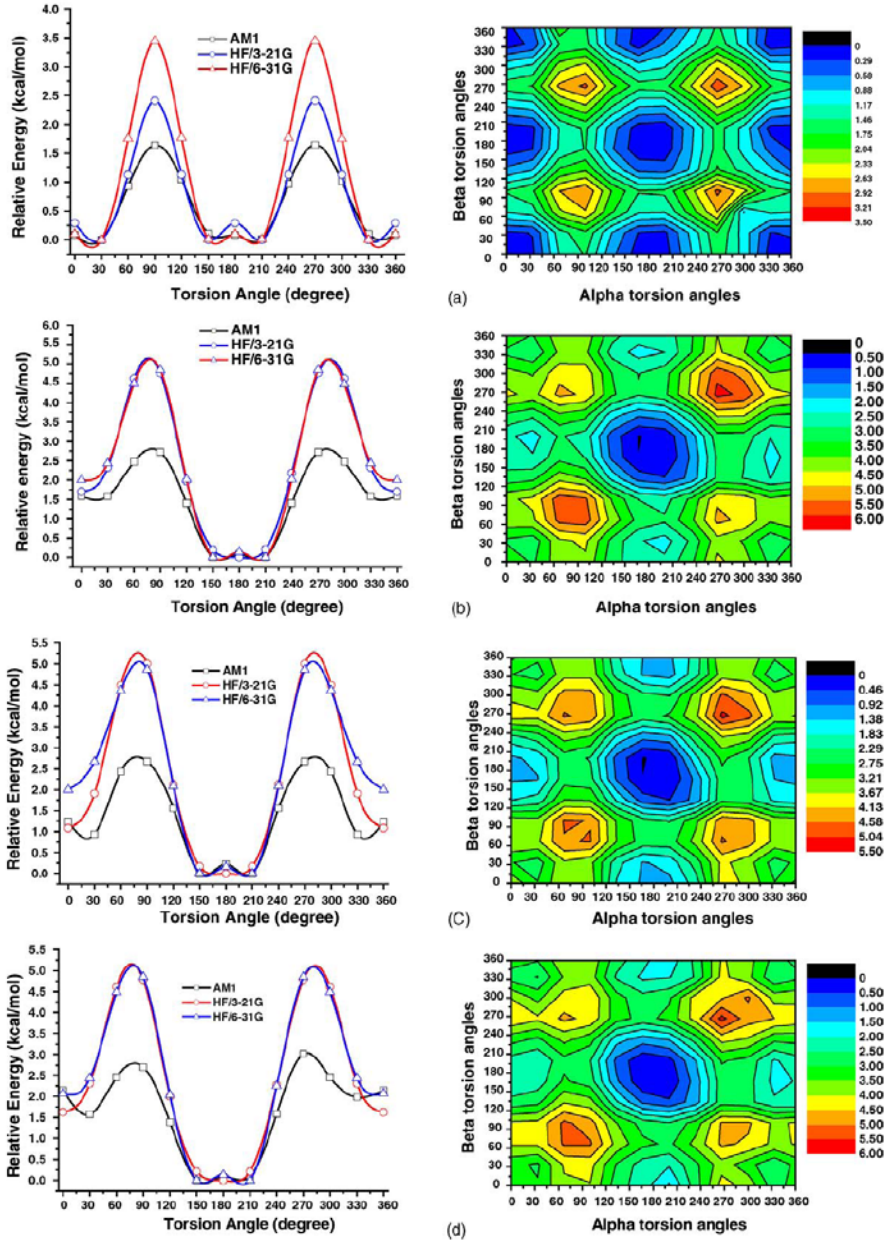

Fig. 2. Potential energy surfaces for OPV_2 alkoxy derivatives with the torsion angle ∠C3-C4-C7-C8 of vinylene units and potential energy hypersurfaces for OPV_2 with the α torsion angle (∠C3-C4-C7-C8) and β torsion angle (∠C7-C8-C9-C14) of vinylene units: (a) OPV_2, (b) DMO-OPV_2, (c) DHO-OPV_2 and (d) MEH-OPV_2, obtained from HF/3-21G calculation.

Table 1
Structural parameters of OPV_N, obtained from full optimization by the semiempirical (AM1) method and Hartree-Fock (HF/3-21G) method (bond-lengths in (Å), angles in (°))

Structural parameters	OPV_N		DMO-OPV_N		DHO-OPV_N		MEH-OPV_N	
	AM1	HF/3-21G	AM1	HF/3-21G	AM1	HF/3-21G	AM1	HF/3-21G
R(H′–H1)	2.39	2.37	–	–	–	–	–	–
R(H–O)	–	–	2.34	2.24	2.34	2.24	2.34	2.26
Angle								
∠C3-C4-C7	118.9	118.8	118.8	118.8	120.0	118.9	118.90	118.9
∠C4-C7-C8	124.7	125.9	124.5	125.9	124.6	125.9	125.60	125.6
Torsional angle								
∠C3-C4-C7-C8	159.7	159.6	159.3	179.6	159.2	174.1	161.8	172.5
∠C7-C8-C9-C10	20.1	20.6	21.5	0.6	21.6	6.8	24.1	5.0

weak hydrogen bond interaction occurs for the OPV_N derivatives, as illustrated in Fig. 3(b). Such intramolecular interaction induces that the geometry of OPV_N derivatives is close to planarity (Fig. 3(a)).

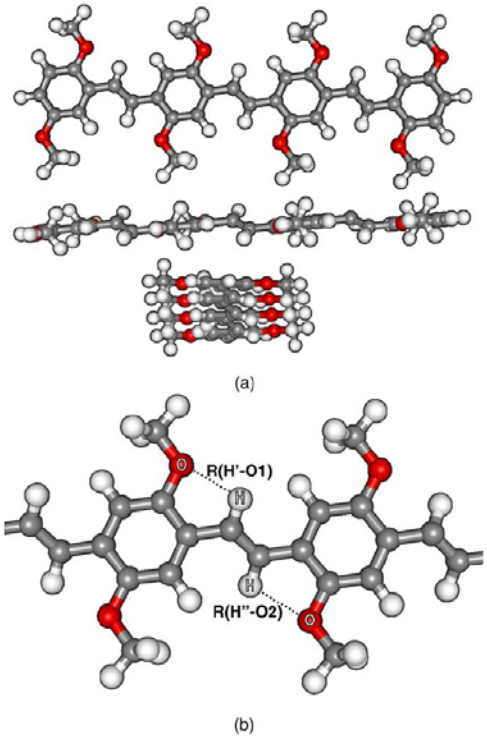

Fig. 3. Schematic representation of intramolecular interaction in the structure of the oligomers of DMO-OPV_N, inducing the coplanar structure. Topview and side view. Intramolecular H-bond interaction occurrance, R(H′–O1) and R(H″–O2) equals to 2.34 Å.

3.3. Electronic properties of OPV_N and OPV_N derivatives

Extrapolated energy gaps of OPV_N and its derivatives were evaluated by excitation energy plots as obtained from TDDFT (B3LYP/6-31G//AM1, B3LYP/6-31G*//AM1, B3LYP/6-31G//HF/3-21G and B3LYP/6-31G*//HF/3-21G) calculations. The calculated results were plotted against the inverse chain length ($1/N$) and extrapolated to infinity. The predicted excitation energies at different levels of calculation are presented in Table 2, together with the results obtained from experiments [41,42].

It was found that the largest transition probabilities are the transition from the ground-state to first excited state ($S_0 \rightarrow S_1$). The energy gaps have been extrapolated against the reciprocal number of units ($1/N$). All plots show excellent linearity as indicated by a high r^2. The extrapolated energy gaps ($Eg_{N\rightarrow\infty}$) of OPV_N and its derivatives obtained from the TDDFT calculations (B3LYP/6-31G//AM1, B3LYP/6-31G*//AM1, B3LYP/6-31G//HF/3-21G and B3LYP/6-31G*//HF/3-21G) were then predicted and the results are shown in Table 2. The predicted energies are consistently lower than the experimental values for each of the OPV_N derivatives, which are 2.38, 2.18, 2.08 and 2.10 eV, respectively. It was found from our study that the energy gaps of OPV_N obtained from density functional theory based on the geometry from HF/3-21G (TDDFT(B3LYP/6-31G//HF/3-21G) and TDDFT(B3LYP/6-31G*//HF/3-21G) are in good agreement with the experiments. However, the energy gaps of DMO-OPV_N, DHO-OPV_N and MEH-OPV_N are overestimated by about 0.3 eV. This observation was the found inherent in the TDDFT calculations [24–26]. Another fact is that the predicted energy gaps were evaluated for the isolated gas-phase chains, while the experimental energy gaps were measured in liquid phase where the environmental influence and the interchain interactions are involved [29–33].

Recently, Zhan et al. [43,44] found that there is a simple linear relationship between experimental values and calculated excitation energies. The linear relationship can be

Table 2
TDDFT excitation energies of oligomers with B3LYP functional and two basis sets (6-31G and 6-31G*), based on the ground-state geometries obtained from AM1 and HF/3-21G methods

Oligomer	TDDFT			
	(B3LYP/6-31G//AM1)	(B3LYP/6-31G*//AM1)	(B3LYP/6-31G//HF/3-21G)	(B3LYP/ 6-31G*//HF/3-21G)
OPV_N				
$N=2$	4.19	4.10	4.41	4.32
$N=3$	3.43	3.36	3.73	3.66
$N=4$	3.07	3.00	3.39	3.32
$N=5$	2.86	2.80	3.19	3.12
$N=6$	2.74	2.64	3.06	2.99
	($r^2=1.000$)	($r^2=1.000$)	($r^2=1.000$)	($r^2=1.000$)
Eg ($N=\infty$)	2.01	1.90	2.38	2.32
Experimental			2.38[a]	
DMO-OPV_N				
$N=2$	3.55	3.47	3.59	3.54
$N=3$	3.02	2.94	3.14	3.05
$N=4$	2.75	2.65	2.76	2.73
$N=5$	2.58	2.51	2.64	2.59
$N=6$	2.46	2.41	2.53	2.48
	($r^2=0.998$)	($r^2=0.998$)	($r^2=0.992$)	($r^2=0.997$)
Eg ($N=\infty$)	1.93	1.87	2.01	1.95
Experimental			2.18[b]	
DHO-OPV_N				
$N=2$	3.53	3.46	3.59	3.51
$N=3$	3.00	2.93	3.04	2.97
$N=4$	2.70	2.63	2.73	2.67
$N=5$	2.55	2.48	2.57	2.51
	($r^2=0.998$)	($r^2=0.998$)	($r^2=0.999$)	($r^2=0.999$)
Eg ($N=\infty$)	1.89	1.82	1.89	1.83
Experimental			2.08[b]	
MEH-OPV_N				
$N=2$	3.54	3.47	3.59	3.52
$N=3$	3.00	2.94	3.04	2.98
$N=4$	2.72	2.65	2.75	2.69
$N=5$	2.56	2.49	2.59	2.52
	($r^2=0.999$)	($r^2=0.999$)	($r^2=0.998$)	($r^2=0.999$)
Eg ($N=\infty$)	1.90	1.83	1.92	1.86
Experimental			2.10[b]	

[a] Reference [41].
[b] Reference [42].

used to semiquantitatively estimate the lowest excitation energies by partially reducing the systematic errors [26]. The value of the slope multiplying the calculated transition energy is greater than 1.0 showing that the differences increase with increasing excitation energies. At the calculated TDDFT values tend to be smaller than the experimental values by 0.3 eV. This effect can be clearly seen from the fits in Table 3. We obtained the linear relationship shown in Table 3 for the correction the of extrapolated energy gaps of DMO-OPV_N, DHO-OPV_N and MEH-OPV_N. The predicted estimated energy gaps are set up from linear relationship between the experimental values and calculated excitation energies obtained from TDDFT methods (B3LYP/6-31G//AM1, B3LYP/6-31G*//AM1, B3LYP/6-31G//HF/3-21G and B3LYP/6-31G*//HF/3-21G) as shown in Table 3.

The values of the linear correlation coefficient in Table 3 can be used to summarize the above discussions. The linear fits between the calculated and experimental values for the excitation energies based on the ground-state geometries from AM1 and HF/3-21G methods are summarized

Table 3
Linear fits between the calculated and experimental values for the excitation energies based on the ground-state geometries from AM1 and HF/3-21G methods

Methods	Linear equation	Linear correlation coefficient
TDDFT(B3LYP/6-31G//AM1)	$E_{expt}=2.518E_{TD}-2.682$	0.999(7)
TDDFT(B3LYP/6-31G*//AM1)	$E_{expt}=3.537E_{TD}-4.375$	0.910(8)
TDDFT(B3LYP/6-31G//HF/3-21G)	$E_{expt}=0.604E_{TD}+0.947$	0.991(2)
TDDFT(B3LYP/6-31G*//HF/3-21G)	$E_{expt}=0.604E_{TD}+0.983$	0.991(2)

in Table 3. For the TDDFT calculations at each level of theory, the linear correlation relationship between the calculated and experimental values as good as the linear. The correlation coefficients based on the TDDFT calculations using the HF geometry (at the TDDFT(B3LYP/6-31G)//HF/3-21G and TDDFT(B3LYP/6-31G*)//HF/3-21G levels) are closer to unity than those at the AM1 geometry (at the TDDFT(B3LYP/6-31G)//AM1 and TDDFT(B3LYP/6-31G*)//AM1 levels). It is indicated that the HF/3-21G level is giving better geometry results as compared to the AM1 level.

The coefficients at the HF/3-21G geometry, TDDFT (B3LYP/6-31G)//HF/3-21G (E_{expt}=0.604$E_{TDDFT\text{-}B3LYP/6\text{-}31G}$ + 0.947) and TDDFT(B3LYP/6-31G*)//HF/3-21G methods (E_{expt} = 0.604$E_{TDDFT\text{-}B3LYP/6\text{-}31G^*}$ + 0.983), differ slightly. The basis set dependence of the TDDFT results shows that the economical 6-31G* basis set is not generally sufficient for calculating the excitation energies for use in correlating with molecular properties. The values of the linear relationship at all levels, TDDFT(B3LYP) levels of theory, do not depend on the basis sets (6-31G and 6-31G*) for calculated the excitation energies. Recently, Parac et al. [45] conducted a comprehensive study of the lowest excitation energies of polycyclic aromatic hydrocarbons by TDDFT calculations. They are shown linear least squares fit of the B3LYP calculation. The coefficient of Parac et al. data $E_{expt} = 1.03E_{calc.} + 0.06$ (R = 0.970) and $E_{expt} = 1.11E_{calc.} - 0.64$ (R = 0.941) for singlet L_a and L_b states, respectively, is closer to unity. From Parac results, we can suggest that Dunning's cc-pVTZ basis sets [46,47] could in principle be employed for improve the results. Due to the correlation-consistent polarized valence triple zeta (cc-pVTZ) basis sets developed by Dunning have been used to assure that the effects from the polarization functions are treated. These basis sets are specifically designed for high quality calculations using correlation methods.

4. Conclusions

The structural and electronic properties of OPV_N and derivatives were studied, based on quantum-chemical calculations. A conformational study of OPV_2 and alkoxy derivatives by AM1, HF/3-21G and HF/6-31G calculations demonstrate that these derivatives prefer a coplanar structure due to weak hydrogen bonds between the oxygen atom of the substituted alkoxy groups and the hydrogen atom of the vinylene linkage. Based on our results, it is found that the energy gaps decrease in the order of OPV_N > DMO-OPV_N > MEH-OPV_N > DHO-OPV_N. Therefore, it can be concluded that the oligomers with increasingly bulky substituents such as OCH_3, OC_6H_{17} and $OC_2H_3(C_2H_5)(C_4H_9)$ result in decreased energy gaps, compared to OPV_N. The oxygen atom of the hexoxy group is more electron-donating than the methoxy groups, the red shift caused by the hexoxy group is significantly larger than the methoxy group. The symmetric substitutions on OPV_N by alkoxy groups (DMO-OPV_N and DHO-OPV_N) cause an insignificant shift in the excitation energies compared to that of original OPV_N and unsymmetric substitutions on OPV_N (MEH-OPV_N). It is important to note that the electronic properties of OPV_N and alkoxy substituted-OPV_N depend on the symmetric substitutions on OPV_N and the size of the side chain. The electronic effects from the alkoxy side chains play an important role in the electronic property of poly (*para*-phenylenevinylene).

These linear relationships can be employed to semiquantitatively estimate first excitation energy. We introduce the relationships with the working function of $E_{expt} = 0.604E_{TDDFT\text{-}B3LYP/6\text{-}31G} + 0.947$ and $E_{expt} = 0.604E_{TDDFT\text{-}B3LYP/6\text{-}31G^*} + 0.983$, based on the geometry obtained from HF/3-21G for corrected the extrapolated energy gaps of DMO-OPV_N, DHO-OPV_N and MEH-OPV_N. It was found that the TDDFT method in combination with a simple linear relationship can be used to predict the lowest excitation energies. The trends in energy gaps observed for OPV_N and its derivatives may be useful for the design of novel conducting polymer materials. In addition, the TDDFT method with B3LYP functional can be applied to large molecular systems such as OPV_N derivatives and the correction for the excitation energies is required in order to obtain reliable energetic properties.

Acknowledgment

The authors thank Prof. Alfred Karpfen and Prof. Peter Wolschann for valuable discussion and suggestions. This work is supported by the Royal Golden Jubilee Ph.D. Program (3C.KU/46/B.1). S.H. is grateful to the Thailand Research Fund for basic research grant (RSA4780007) and S.S. is grateful to the Graduate School, KU, for partial support via Grant-in-Aid for his thesis. T.K. and T.S. thank MTEC for supporting the organic light emitting device project. Generous supply of computing time and research facilities by the Postgraduate Education and Research Programs in Petroleum and Petrochemical Technology, LCAC and the Computing Center of KU is gratefully acknowledged. Thanks are also due to Anthony Reardon for reading the manuscript.

References

[1] C.K. Chiang, C.R. Fincher Jr., Y.W. Park, A.J. Heeger, H. Shirakava, E.J. Louis, S.C. Gau, A.G. MacDiarmid, Phys. Rev. Lett. 39 (1977) 1098–1101.
[2] J.H. Burroughes, D.D.C. Bradley, A.R. Brown, R.N. Marks, K. Mackay, R.H. Friend, P.L. Burn, A.B. Holmes, Nature 347 (1990) 539–541.
[3] D. Braun, A.J. Heeger, Appl. Phys. Lett. 58 (1991) 1982–1984.
[4] P.L. Burn, A.B. Holmes, A. Kraft, D.D.C. Bradley, A.R. Brown, R.H. Friend, R.W. Gymer, Nature 356 (1992) 47–49.
[5] T. Ohnishi, T. Noguchi, T. Nakano, M. Hirooka, I. Murse, Synth. Met. 41 (1991) 309–312.
[6] L. Rodriguez-Monge, J. Phys. Chem. B 102 (1998) 4466–4476.

[7] O. Lhost, J.L. Bredas, J. Chem. Phys. 96 (1992) 5279–5288.
[8] A. Pogantsch, G. Heimel, E. Zojer, J. Chem. Phys. 117 (1992) 5921–5928.
[9] V. Chernyak, S.N. Volkov, S. Mukamel, J. Phys. Chem. A 105 (2001) 1988–2004.
[10] M. Loegdlund, P. Dannetun, C. Fredriksson, W.R. Salaneck, J.L. Bredas, Synth. Met. 67 (1994) 141–145.
[11] F. Negri, G. Orlandi, J. Mol. Struct. 521 (2000) 197–209.
[12] S. Hirata, M. Head-Gordon, R.J. Bartlett, Chem. Phys. Lett. 314 (1999) 291–299.
[13] D. Beljonne, Z. Shuai, R.H. Friend, J.L. Bredas, J. Chem. Phys. 102 (1995) 2042–2049.
[14] J.L. Bredas, Adv. Mater. 7 (1995) 263–274.
[15] J.B. Foresman, M. Head-Gordon, J.A. Pople, J. Phys. Chem. 96 (1992) 135–149.
[16] K.B. Wiberg, A.E. de Oliveira, G. Trucks, J. Phys. Chem. 106 (2002) 4192–4199.
[17] C. Jamorski, M.E. Casida, D.R. Salahub, J. Chem. Phys. 104 (1996) 5134–5147.
[18] E.K.U. Gross, W. Kohn, Adv. Quant. Chem. 21 (1990) 255–291.
[19] R. Bauernschmitt, R. Ahlrichs, Chem. Phys. Lett. 256 (1996) 454–464.
[20] M.E. Casida, C. Jamorski, K.C. Casida, D.R. Salahub, J. Chem. Phys. 108 (1998) 4439–4449.
[21] K.B. Wiberg, R.E. Stratmann, M.J. Frisch, Chem. Phys. Lett. 297 (1998) 60–64.
[22] O. Kwon, M.L. McKee, J. Phys. Chem. A 104 (2000) 7106–7112.
[23] Y. Gao, C. Liu, Y. Jiang, J. Phys. Chem. A 106 (2002) 5380–5384.
[24] G. Zhang, J. Ma, S. Li, Y. Jiang, Macromolecules 35 (2002) 1109–1115.
[25] G. Zhang, J. Ma, S. Li, Y. Jiang, Macromolecules 36 (2003) 2130–2140.
[26] J.S.K. Yu, W.C. Chen, C.H. Yu, J. Phys. Chem. A 107 (2003) 4268–4275.
[27] J. Ma, S. Li, Y. Jing, Macromolecules 35 (2002) 1109–1115.
[28] A.F. Diaz, J. Crowley, J. Bargon, G.P. Gardini, J.B. Torrance, J. Electroanal. Chem. 121 (1981) 355–361.
[29] P. Gomes de Costa, R.G. Dandrea, E.M. Conwell, Phys. Rev. B 47 (1993) 1800–1810.
[30] M. Rohlfing, S.G. Louie, Phys. Rev. Lett. 82 (1999) 1959–1962.
[31] R.B. Capaz, M.J. Caldas, Phys. Rev. B 67 (2003) 205205–205209.
[32] A. Ferretti, A. Ruini, E. Molinari, M.J. Caldas, Phys. Rev. Lett. 90 (2003) 086401–086404.
[33] G. Zheng, S.J. Clark, S. Brand, R.A. Abram, J. Phys.: Condens. Mater. 16 (2004) 8609–8620.
[34] J. Cornil, B. Beljonne, J.L. Bredas, J. Chem. Phys. 103 (1995) 834–841.
[35] SciVision, 200 Wheeler Road, Burlington, MA 01803, USA, http://www.scivision.com.
[36] M.J.S. Dewar, E.G. Zoebisch, E.F. Healy, J.J.P. Stewart, J. Am. Chem. Soc. 107 (1985) 3902–3909.
[37] M.J. Frisch, G.W. Trucks, H.B. Schlegel, G.E. Scuseria, M.A. Robb, J.R. Cheeseman, V.G. Zakrzewski, J.A. Montgomery, R.E., Jr. Stratmann, J.C. Burant, S. Dapprich, J.M. Millam, A.D. Daniels, K.N. Kudin, M.C. Strain, O. Farkas, J. Tomasi, V. Barone, M. Cossi, R. Cammi, B. Mennucci, C. Pomelli, C. Adamo, S. Clifford, J. Ochterski, G.A. Petersson, P.Y. Ayala, Q. Cui, K. Morokuma, D.K. Malick, A.D. Rabuck, K. Raghavachari, J.B. Foresman, J. Cioslowski, J.V. Ortiz, A.G. Baboul, B.B. Stefanov, G. Liu, A. Liashenko, P. Piskorz, I. Komaromi, R. Gomperts, R.L. Martin, D.J. Fox, T. Keith, M.A. Al-Laham, C.Y. Peng, A. Nanayakkara, M. Challacombe, P.M.W. Gill, B. Johnson, W. Chen, M.W. Wong, J.L. Andres, C. Gonzalez, M. Head-Gordon, E.S. Replogle, J. A. Pople, Gaussian Inc., Pittsburgh, PA, 1995 and 1999.
[38] G. Mao, J.E. Fischer, F.E. Karasz, M.J. Winokur, J. Chem. Phys. 98 (1993) 712–716.
[39] F. Hibbert, J. Emsley, Adv. Phys. Org. Chem. 26 (1990) 255–275.
[40] M. Traetterg, E.B. Frantsen, F.C. Mijlhoff, A. Hoekstra, J. Mol. Struct. 26 (1975) 57–68.
[41] M. Halim, I.D.W. Samuel, E. Rebourt, A.P. Monkman, Synth. Met. 84 (1997) 951–952.
[42] K.F. Voss, C.M. Foster, L. Smilowitz, D. Mihailovic, S. Askari, G. Srdanov, Z. Ni, S. Shi, A.J. Heeger, F. Wudl, Phys. Rev. B 43 (1991) 5109–5118.
[43] C.G. Zhan, J.A. Nichols, D.A. Dixon, J. Phys. Chem. A 107 (2003) 4184–4195.
[44] C.G. Zhan, J.A. Nichols, D.A. Dixon, J. Phys. Chem. A 107 (2003) 10154–10158.
[45] M. Parac, S. Grimme, Chem. Phys. 292 (2003) 11–21.
[46] T.H. Dunning Jr., J. Chem. Phys. 90 (1989) 1007–1023.
[47] R.A. Kendall, T.H. Dunning Jr., R.J. Harrison, J. Chem. Phys. 96 (1992) 6796–6806.

Publication II

Structures, absorption spectra, and electronic properties of polyfluorene and its derivatives: A theoretical study.

Sriwichitkamol, K., Suramitr, S., Poolmaee P., and Hannongbua, S.

J. Theor. Comp. Chem. 2006, 5, 595-608.

Journal of Theoretical and Computational Chemistry
Vol. 5, No. 3 (2006) 595–608

World Scientific
www.worldscientific.com

STRUCTURES, ABSORPTION SPECTRA, AND ELECTRONIC PROPERTIES OF POLYFLUORENE AND ITS DERIVATIVES: A THEORETICAL STUDY

KRIENGSAK SRIWICHITKAMOL, SONGWUT SURAMITR,
POTJAMAN POOLMEE and SUPA HANNONGBUA*

Department of Chemistry, Faculty of Science
Kasetsart University, Bangkok 10900, Thailand
**fscisph@ku.ac.th*

Received 8 February 2006
Accepted 29 May 2006

The structural and energetic properties of polyfluorene and its derivatives were investigated, using quantum chemical calculations. Conformational analysis of bifluorene was performed by using *ab initio* (HF/6-31G* and MP2/6-31G*) and density functional theory (B3LYP/6-31G*) calculations. The results showed that the local energy minimum of bifluorene lies between the coplanar and perpendicular conformation, and the B3LYP/6-31G* calculations led to the overestimation of the stability of the planar pi systems. The HOMO-LUMO energy differences of fluorene oligomers and its derivatives — 9,9-dihexylfluorene (DHPF), 9,9-dioctylfluorene (PFO), and bis(2-ethylhexyl)fluorene (BEHPF) — were calculated at the B3LYP/6-31G* level. Energy gaps and effective conjugation lengths of the corresponding polymers were obtained by extrapolating HOMO-LUMO energy differences and the lowest excitation energies to infinite chain length. The lowest excitation energies and the maximum absorption wavelength of polyfluorene were also performed, employing the time-dependent density functional theory (TDDFT) and ZINDO methods. The extrapolations, based on TDDFT and ZINDO calculations, agree well with experimental results. These theoretical methods can be useful for the design of new polymeric structures with a reducing energy gap.

Keywords: Polyfluorene; quantum chemical calculations; conductive polymer; time-dependent density functional theory; energy gap; absorption spectra.

1. Introduction

Since the first report of electroluminescence in a conjugated polymer,[1] many experimental and theoretical efforts have been devoted to improving the performance of polymer-based light-emitting devices.[2] Low-resolution matrix displays have now reached the stage of commercialization.[3] Conjugated polymers are also widely investigated for use in organic transistors,[4–6] as well as in photodiodes and solar cells[7–9] where light is absorbed by the material and converted into an electric current. However, these devices usually suffer from the low charge mobilities achieved in

polymer films.[5] Poly(para-phenylenevinylene) (PPV) was the first polymer involved in light-emitting devices.[1,10] Interest has now shifted to polymers of high purity and high stability in view of commercial applications. Photoluminescent and electroluminescent properties of a variety of conjugated polymers have been intensively investigated in search of new, highly efficient light-emitting device materials for the three primary colors: red, green, and blue. Of these conjugated polymers, polyphenylenes are attractive candidates for blue light-emitting materials because of their large energy gaps.[11–15] The first blue light-emitting device was fabricated with poly(9,9-dihexylfluorene), emitting light with a peak at 470 nm (corresponding to 2.6 eV of photon energy).[11] Poly(para-phenylene) was immediately introduced as another blue light-emitting material, suggesting that light emission might be a general feature of conjugated polymers.[12,13] Blue light emitters have also been obtained by controlling the conjugation length along the conjugated backbones, e.g. attaching bulky side groups to turn color by introducing steric distortion of the conjugated chain.[16–19]

Fluorene derivatives present an interesting alternative to blue light-emitting materials. Indeed, fluorenes and oligofluorenes are well known as highly fluorescent compounds.[11] These molecules contain a rigidly planar biphenyl structure in the fluorene monomer unit with facile functionalization at the C(9) position, offering the prospect of controlling the polymer solubility and other physical properties. Moreover, the remote substitution at C(9) does not induce steric effects with adjacent aromatic rings. In this regard, various fully conjugated polyfluorenes have been studied for light-emitting device applications. However, the formation of excimers has been observed in these fully conjugated polymers, thus limiting their utilization in optical devices.

The calculated highest occupied molecular orbital-lowest unoccupied molecular orbital (HOMO-LUMO) gap agrees fairly well with the experimental energy gap in many cases.[19–23] It is desirable to obtain more rigorous information on the nature of the lowest singlet excited state by employing more elaborate theoretical methods. The implicit assumption underlying this approximation is that the lowest singlet excited state can be described by only one singly excited configuration, in which an electron is promoted from the highest occupied molecular orbital (HOMO) to the lowest unoccupied molecular orbital (LUMO). In addition, the orbital energy difference between HOMO and LUMO is still an approximate to the transition energy, since the transition energy also contains significant contributions from some two-electron integrals. However, the real situation is that an accurate description of the lowest singlet excited state requires a linear combination of a number of excited configurations, although the one mentioned above often plays a dominant role.

There are a variety of theoretical approaches for evaluating the lowest singlet excited state for oligomers and infinite polymers. The crudest estimate is the orbital energy difference between HOMO and LUMO, obtained from density functional theory (DFT) calculations. Hartree–Fock (HF)-based methods such as configuration interaction singles (CIS) and random phase approximation usually

only provide qualitative or semi-qualitative descriptions for the low-lying excited states. Time-dependent density functional theory (TDDFT) is a recently developed method for calculating excitation energies. A significant quantitative improvement in the excitation energies from TDDFT over those from HF-based methods has been demonstrated.[19,20]

2. Method of Calculations

The ground state geometries of oligomers were fully optimized using DFT at the B3LYP/6-31G* level, as implemented in Gaussian 98. ZINDO and TDDFT (B3LYP/6-31G*) calculations of the lowest excitation energies and the maximal absorption wavelengths (λ_{abs}) were then performed at the optimized geometries of the ground states. A conformational analysis of bifluorene was carried out by changing the torsional angle from 0° to 180° in steps of 15°. The geometries were optimized at the HF, MP2, and B3LYP levels with the 6-31G* basis set. The linear extrapolation technique was employed in this research. The linearity between the calculated energy gap, maximal absorption wavelengths of the oligomers, and the reciprocal chain length is excellent for this homologous series of oligomers. Thus, these values for the polymers can be obtained by extrapolating the resultant linear relationship to infinite chain length. In addition, the effective conjugation length (ECL) was estimated by the convergence of the excitation energies with the chain length within a threshold of 0.01 eV, based on the obtained linearity between the excitation energy and reciprocal chain length. The Fluorine derivatives 9,9-dihexylfluorene (DHPF), 9,9-dioctylfluorene (PFO), and bis(2-ethylhexyl)fluorene (BEHPF) were investigated in terms of their HOMO-LUMO energy gap and excitation energy, using a similar approach as the one described for Fluorine oligomers.

3. Results and Discussion

3.1. *Structural properties of ground state*

The oligomers' structural properties of polyfluorene $(F)_n$, calculated at the B3LYP/6-31G* level, are given below. Figure 1 shows the sketch map of the polyfluorene structure and Table 1 shows the optimized geometrical parameters of polyfluorene. The results of the optimized structures for the oligomeric molecules of $(F)_n$ ($n = 1-4, 6, 8$) indicate that there is a slight structural change as the chain length n increases. [However, $(F)_3$ has a larger dihedral angle of 0.36° in the five-membered ring $\Phi(2, 3, 4, 9)$ than the average 0.13° in the serial $(F)_n$.] For example, $r(1, 2)$ is $(1.521 \pm 0.001) \times 10^{-10}$ m and the value of $\theta(2, 1, 9)$ is $102.72 \pm 0.02°$ in the series of $(F)_n$. This suggests that the basic structures of the polymers can be described as their oligomers. Additionally, the optimized geometrical parameters are in good agreement with X-ray data.[24] Thus, the structure of $(F)_n$ is dramatically twisted in the five-membered ring, as seen in Fig. 2.

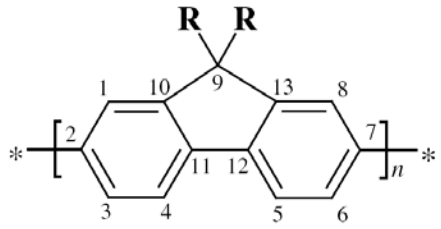

R = H, polyfluorene.
R = dihexyl, poly(9,9-dihexylfluorene) (DHPF).
R = dioctyl, poly(9,9-dioctylfluorene) (PFO).
R = bis(2-ethylhexyl), poly(bis(2-ethylhexyl)fluorene) (BEHPF).

Fig. 1. Sketch map of the polyfluorene structure.

Table 1. Optimized geometrical parameters distance (r), bond angle (θ) and bond torsional angle (Φ), of oligomers $(F)_n$.

	$(F)_n$					
n	1	2	3	4	6	8
$r(1,9)$	1.520	1.521	1.521	1.521	1.521	1.521
$r(11,12)$	1.472	1.470	1.468	1.468	1.468	1.468
$r(4,11)$	1.399	1.398	1.399	1.399	1.399	1.399
$r(3,4)$	1.400	1.397	1.397	1.397	1.397	1.397
$r(2,3)$	1.403	1.412	1.412	1.413	1.413	1.413
$r(1,2)$	1.404	1.413	1.414	1.414	1.414	1.414
$r(1,10)$	1.393	1.389	1.389	1.389	1.389	1.389
$r(10,11)$	1.416	1.416	1.416	1.417	1.416	1.417
$\theta(1,2,3)$	110.04	110.03	109.95	109.95	109.95	109.94
$\theta(2,3,4)$	108.60	108.55	108.70	108.69	108.69	108.70
$\theta(2,1,9)$	102.74	102.73	102.71	102.71	102.71	102.71
$\theta(9,4,5)$	120.37	119.82	119.83	119.83	119.82	119.85
$\theta(4,5,6)$	118.93	119.21	119.19	119.19	119.20	119.18
$\theta(5,6,7)$	120.65	121.63	121.65	121.65	121.66	121.63
$\Phi(1,2,3,4)$	0.000	0.042	0.289	0.316	0.403	0.399
$\Phi(2,3,4,9)$	0.000	0.191	0.359	0.025	0.134	0.154
$\Phi(4,5,6,7)$	0.000	0.012	0.093	0.118	0.178	0.154

3.2. *Conformational analysis*

The torsion potential energy curves of bifluorene obtained through various methods are displayed in Fig. 3. The overall shape of the torsion potential energy curve obtained from HF is quite similar to that from MP2. The minimum-energy conformations in the free molecule are nearly in the middle of the coplanar and perpendicular conformations. Both methods predict that the coplanar energy barrier is higher than the perpendicular energy barrier. The torsion angle constitutes a compromise between the effect of π electron conjugation (which favors a planar conformation) and steric interaction of *ortho*-hydrogen atoms (which favors a non-planar

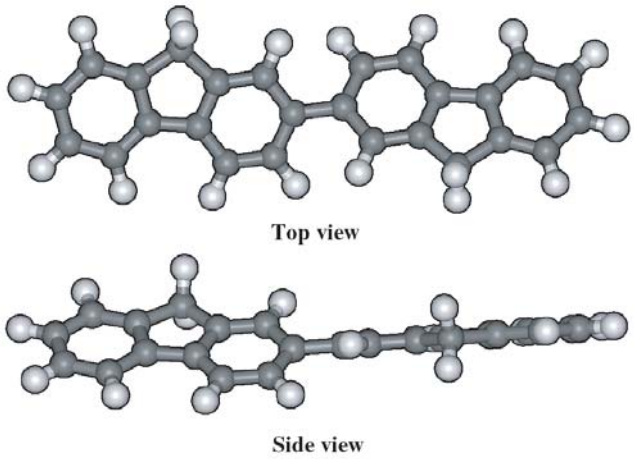

Fig. 2. Torsion units of optimized structures for $(F)_n$.

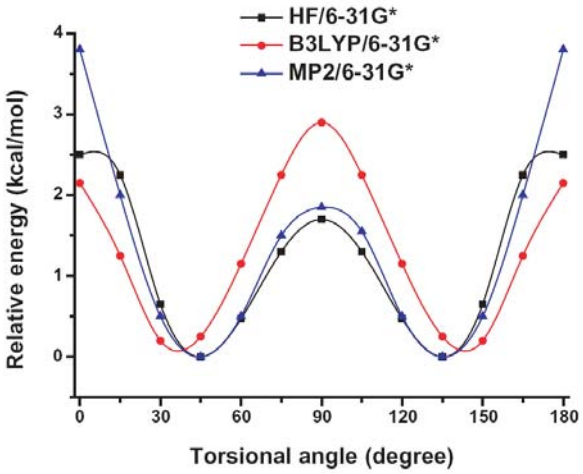

Fig. 3. Torsion potential energy curves of bifluorene obtained by HF, MP2, and B3LYP calculations.

conformation). The MP2 correlation effect on the rotational barriers is not significant in the case of bifluorene, with larger increments in the coplanar energy barrier and smaller increments in the perpendicular energy barrier. On the other hand, B3LYP gives the reverse result: the perpendicular energy barrier is largely increased and the coplanar energy barrier is largely reduced. The calculated equilibrium torsion angle is 37.6°, which is in good agreement with the theoretical results obtained from HF/STO-3G (i.e. 38.7°). The conjugated effect on the rotational barriers is remarkable, as predicted by B3LYP.

The energy barriers from the equilibrium geometries towards the coplanar conformation and perpendicular conformation, as well as the differences between them,

Table 2. The coplanar energy barriers ΔE_1, perpendicular energy barriers ΔE_2, and the difference between them ($\Delta E_2 - \Delta E_1$); all in kcal/mol.

Methods	The Relatives Energy (kcal/mol)		
	ΔE_1	ΔE_2	$\Delta E_2 - \Delta E_1$
HF/6-31G*	3.48	1.70	−1.78
B3LYP/6-31G*	3.90	1.94	−1.96
MP2/6-31G*	2.14	2.93	0.79

are listed in Table 2. The electron correlation corrections to the self-consistent field torsion potentials from B3LYP are dramatically different from those of the MP2 approximation in bifluorene: they have different signs ($\Delta E_2 - \Delta E_1$), as was pointed out by Karpfen *et al.*[23] in their study on various conjugated and non-conjugated systems. Note that the electron correlation contributions are largely different at different torsion angles, due to the partial bond-breaking of conjugated single bonds by internal rotations. The extreme higher perpendicular and lower coplanar energy barriers of bifluorene obtained via B3LYP calculations were attributed to the overestimation of the stability of the planar π systems DFT methods.[23] On the other hand, it was found that the DFT approach provides a good description of the conformational properties of oligo- and poly-thiophenes, which is in satisfactory agreement with the experimental evidence.[25]

3.3. *Front molecular orbitals*

It is useful to examine the highest occupied orbitals and the lowest virtual orbitals for these oligomers and polymers, so as to provide the framework for the excited state calculations (using TDDFT) in the subsequent section. We have found that the relative ordering of the occupied and virtual orbitals provides a reasonable qualitative indication of the excitation properties. The HOMO orbitals and LUMO orbitals of the bifluorene $(F)_2$ by B3LYP/6-31G* are shown in Fig. 4. Interestingly, the main characters of the front orbitals by HF/3-21G* are the same as those by B3LYP /6-31G*.

As shown in Fig. 4, the HOMO and LUMO of the $(F)_2$ molecule are predominantly localized on the phenyl rings. There is antibonding between the bridge atoms and bonding between the bridge carbon atom and its conjoint atoms in the same benzene in the HOMO. In contrast, there is bonding in the bridge single bond and antibonding between the bridge atom and its neighbor in the same phenyl ring in the LUMO.

3.4. *HOMO-LUMO gaps and the lowest excitation energies*

It is well known that the energy gap of the polymer $(M)_n$ is the orbital energy difference between the highest occupied molecular orbital (HOMO) and the lowest

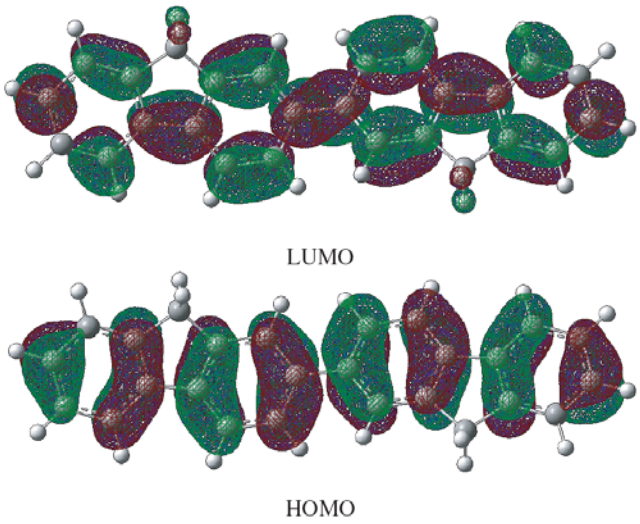

Fig. 4. HOMO and LUMO orbitals of the $(F)_2$ molecule.

unoccupied molecular orbital (LUMO), when $n = \infty$. However, it is difficult to obtain the correct data by experiment due to the experimental condition limit, such as interchain interactions, solvent effects, and so on. The experimental energy gap is usually observed by two methods: the maximal wavelength in the spectra or the onset from CV-UV.[26] These methods are valid when the lowest singlet excited state can be described by only one singly excited configuration, in which an electron is promoted from HOMO to LUMO; in such a situation, the experimental condition limit can be neglected. Our HOMO-LUMO gaps have been obtained from density functional theory (DFT) calculations. We also calculated the lowest excitation energies of the oligomers, and compared them with the experiment data to extrapolate the energy gap. Time-dependent DFT (TDDFT) and ZINDO calculations were employed to examine the low-lying singlet excited states of the oligomers. The HOMO-LUMO gaps ($\Delta_{(H-L)}$), the lowest excitation energies (E_g) of the oligomers, and the extrapolated energy gaps of polyfluorene are presented in Table 3. There is a good linear relationship between the HOMO-LUMO gaps, the lowest excitation energies, and the inverse chain length (see Fig. 5).

In the plot, we can extrapolate the HOMO-LUMO gaps to infinite chain length to get 3.33 eV to polyfluorene. This value is close to the experiment data, i.e. 2.97 eV to polyfluorene. Therefore, it is possible to obtain useful information on the nature of the lowest singlet excited state by employing the HOMO-LUMO gap. This approach can also be used to provide valuable information on estimate energy gaps of oligomers and polymers, especially even larger systems.[27] However, the orbital energy difference between HOMO and LUMO is still an approximate estimate to the transition energy, since the transition energy also contains significant

Table 3. The lowest TDDFT and ZINDO excitation energies, the negative of HOMO energies ($-\varepsilon_{\mathrm{HOMO}}$), and HOMO-LUMO gaps of oligomers $(\mathrm{F})_n$; all in eV.

Oligomer $(\mathrm{F})_n$	TDDFT	ZINDO	$-\varepsilon_{\mathrm{HOMO}}$	$\Delta_{\mathrm{H-L}}$
$n = 1$	4.75	4.44	5.80	5.10
$n = 2$	3.87	3.79	5.38	4.21
$n = 3$	3.52	3.60	5.24	3.90
$n = 4$	3.36	3.46	5.17	3.76
$n = 6$	3.22	3.39	5.12	3.63
$n = 8$	3.17	3.35	5.09	3.58
E_g $(n = \infty)$	2.91	3.18	4.98	3.33
Expt.	2.97[a]	2.88[b]		

[a]Our experimental data on polyfluorene film prepared from chloroform solution.
[b]See Ref. 27.

contributions from some two-electron integrals. The real situation is that an accurate description of the lowest singlet excited state requires a linear combination of a number of excited configurations.

To get some useful information for the experiment of the energy gaps, we turn to the spectrum methods. A long-wavelength transition with large oscillator strength (> 0.7) was obtained in this study, thus implying a strong transition. Good agreement is found between the observed E_g values and the E_g values calculated by both TDDFT and ZINDO methods, which were obtained by extrapolating the resultant linear relationship to infinite chain length. However, the TDDFT method is better than the ZINDO method in meeting the experimental data. From Table 3, one can see that the TDDFT predictions systematically underestimate the energy gaps of polymers, with an average deviation of about 0.06 eV. Furthermore, for polyfluorene, the TDDFT caculations exceed the experimental data from Ref. 24 by only 0.03 eV, while the results of ZINDO deviate about 0.27 eV. Two factors may be responsible for the error. One is that calculations on a few longer oligomers may be required so that more data can be used in linear regression. Another is that the predicted energy gaps are for isolated gas-phase chains, while experimental energy gaps are measured in the condensed phase where interchain interactions may be significant.

Despite the good agreement between the calculated excitation energies and the experimental data, it is also necessary to check the validity of the excitation energies calculated by TDDFT. The excitation energies calculated by TDDFT with the current exchange-correlation functional are not reliable when the calculated excitation energies are higher than the negative of HOMO energies. The negative of HOMO energies ($-\varepsilon_{\mathrm{HOMO}}$) and the TDDFT excitation energies are displayed in Table 3. The table shows that, in all cases, the TDDFT excitation energies are below the negative of HOMO energies and thus are numerically reliable. In fact, the energy gaps extrapolated by TDDFT are better than the HOMO-LUMO gaps

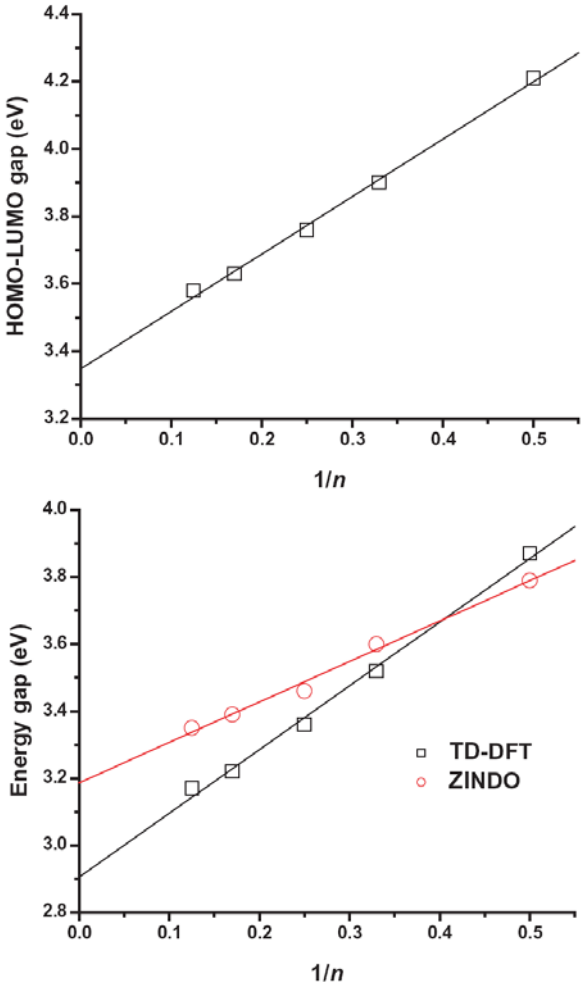

Fig. 5. HOMO-LUMO gaps (up) by B3LYP and the lowest excitation energies E_g (down) by ZINDO and TDDFT, as a function of reciprocal chain length n in oligomers of polyfluorene.

when the experimental data are taken into consideration: the TDDFT calculations deviate from the polyfluorene experimental data by only 0.06 eV, while the HOMO-LUMO gaps deviate by 0.36 eV. Therefore, TDDFT with the B3LYP functional is expected to be a relatively reliable tool for evaluating the excitation energies of low-lying excited states for small- and medium-sized molecules.

In addition, the effective conjugation length (ECL) can be estimated from calculations on a series of oligomers. The effective conjugation length is the repeat unit number at which saturation of a property occurs. The information on the effective conjugation length of polymers is very useful to the synthetic strategies. The ECL for all selected oligomers have been estimated, based on the convergence of the calculated excited energy of the first dipole-allowed excited state with the

increasing chain length. We have taken 0.01 eV as the convergence threshold of tl excitation energies with the chain length, based on the obtained linearity betwe the excitation energy and reciprocal chain length. So, the ECL of polyfluorene estimated at around 14 units.

3.5. *Absorption spectra*

On the basis of the optimized geometry, we calculated the absorption spectrum these oligomers in Table 4. Interestingly, we found that there is a linear relationsh between the macro-absorption and the reciprocal chain length, as seen in Fig. Thus, we list the extrapolating data to $1/n = 0.0$ in the last but one line in Table The results are in good agreement with those from the experiment. Although tl

Table 4. Absorption wavelengths (λ_{abs} in nm) computed using the ZINDO and TDDFT methods, all in nm.

Oligomers $(F)_n$	Absorption Wavelengths (nm)	
n	ZINDO	TDDFT
1	247.9	260.8
2	325.8	320.4
3	346.7	354.2
4	357.1	368.9
6	364.2	384.8
8	369.3	391.1
∞	385.1	349.4
Expt.	383	417.2

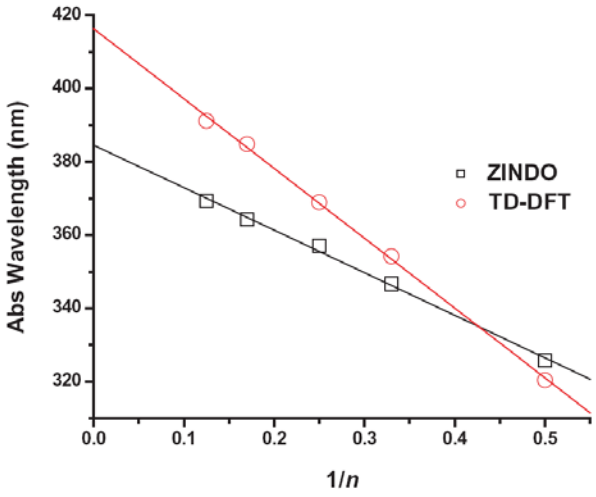

Fig. 6. Absorption wavelengths by ZINDO and TDDFT as a function of $1/n$ in oligomers.

λ_{abs} by ZINDO is shorter than the λ_{abs} by TDDFT for the same molecule, they both have the same trend of increasing as the chain length n increases. The obtained value of 385.1 nm for polyfluorene by ZINDO is close to the experimental data. The λ_{abs} for polyfluorene calculated by TDDFT is slightly longer than the experimental data by 35.2 nm.

3.6. *Electronic properties of polyfluorene derivatives*

For the HOMO-LUMO energy gaps and excitation energies of oligomers of 9,9-dihexylfluorene (DHPF), 9,9-dioctylfluorene (PFO), and bis(2-ethylhexyl) fluorene (BEHPF), we used TDDFT at the B3LYP/6-31G* level — as shown in Table 5 — because this method provides good agreement with the experimental data (electronic energy gap and optical energy gap). The calculated HOMO-LUMO energy gap and excitation energy of 9,9-dihexylfluorene, 9,9-dioctylfluorene, and bis(2-ethylhexyl)fluorene are plotted against inverse chain length and extrapolated to infinity, as shown in Fig. 7. The extrapolated HOMO-LUMO energy gap of poly(9,9-dioctylfluorene) at the B3LYP/6-31G* level was compared with the experimental data from ultraviolet photoelectron spectroscopy (UPS) and X-ray photoelectron spectroscopy (XPS).[28] From the UPS measurement, an ionization potential (IP) of 5.55 eV was obtained; this value is related to the HOMO of polymers in solid states. In comparison, the calculated HOMO of poly(9,9-dioctylfluorene) at the B3LYP/6-31G*//AM1 and B3LYP/6-31G* levels is equivalent to 5.05 eV, which is different from the UPS experimental value by about 0.5 eV. As for the data from the XPS shake-up peak of the C1s core level, the estimated energy gap is 3.2 eV. This value is similar to the calculated energy gap of poly(9,9-dioctylfluorene) obtained at the B3LYP/6-31G*//AM1 and B3LYP/6-31G* levels, $E_g = 3.21$ eV. Thus, the energy gap values of DHPF and BEHPF, which are shown in Table 5 and calculated using the same methods, are in good agreement with the values corresponding to the UPS and XPS experiments.

The excitation energy values, which have been calculated using TDDFT at the same level as the HOMO-LUMO energy gap values (B3LYP/6-31G*), are related to the optical energy gaps from the optical absorption maximum of polymers. TDDFT considers the energy of electrons jumping to the next energy level; therefore, the results from excited energy calculations are different and cannot be compared with

Table 5. HOMO-LUMO energy gaps and excitation energies of DHPF, PFO, and BEHPF; all in eV.

Polymers	HOMO-LUMO Gap	Excitation Energy	E_g(Expt)
DHPF	2.92	2.72	—
PFO	3.21	2.96	3.1–3.2[28]
BEHPF	3.03	2.84	—

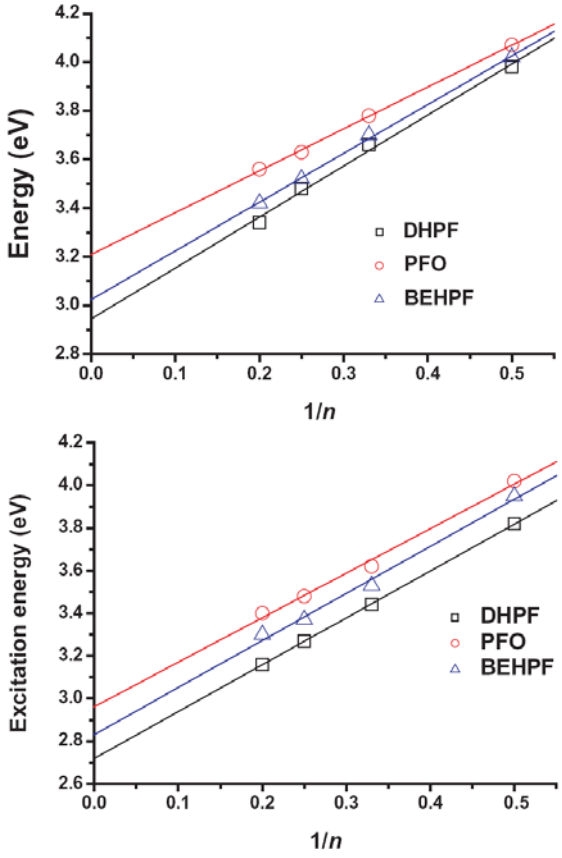

Fig. 7. Plots of calculated energy gaps and excitation energies vs. inverse chain length of the oligomer units and extrapolating to an infinite number of units for DHPF, PFO and BEHPF: HOMO-LUMO gaps (up), excitation energies (down).

the HOMO-LUMO or energy gaps. It was found that the energy values from excited states are smaller than the energy gaps.

4. Conclusion

Conformational analysis of the bifluorene molecule has been performed by using *ab initio* (HF/6-31G* and MP2/6-31G*) and DFT (B3LYP/6-31G*) methods. The results from HF/6-31G* are quite similar to those from MP2/6-31G*. The minimum-energy conformations in the free molecule are nearly in the middle of the co-planar and perpendicular conformations, and both methods predict that the co-planar energy barrier is higher than the perpendicular energy barrier. However, the B3LYP method gives the reverse results: the perpendicular energy barrier is largely increased and the co-planar energy barrier is largely reduced. The chain length dependence of $\Delta_{\mathrm{H-L}}$ has also been studied by employing density functional theory with the B3LYP functional. The extrapolation results of λ_{abs} and E_g are in

good agreement with the experimental data. The fundamental structural and energetic information of bifluorene can be useful for the further design of new polymeric structures with enhanced specific structural properties.

Acknowledgments

This work was supported by the Thailand Research Fund (BRG4780007), Center of Nanotechnology and KURDI. S. Suramitr is grateful to the RGJ Ph.D. Program for a scholarship (3C.KU/46/B.1). LCAC, the computing centers of KU, the Postgraduate on education and research in Petroleum and Petrochemical Technology are gratefully acknowledged for providing software packages and computing time. Thanks are also due to W. J. Holzschuh for the reading of the manuscript.

References

1. Burroughes JH, Bradley DDC, Brown AR, Marks RN, Friend RH, Burn PL, Holmes AB, *Nature* **347**:539–541, 1990.
2. Friend RH, Gymer RW, Holmes AB, Burroughes JH, Marks RN, Taliani C, Bradley DDC, Dos Santos DA, Bredas JL, Logdlund M, Salaneck WR, *Nature* **397**:121–128, 1999.
3. Kalinowski J, *J Phys D: Appl Phys* **32**:R179–R250, 1999.
4. Sirringhaus H, Brown PJ, Friend RH, Nielsen MM, Bechgaard K, Langeveld-Voss BMW, Spiering AJH, Janssen RAJ, Meijer EW, Herwig P, De Leeuw DM, *Nature*, **401**:685–688, 1999.
5. Zhitenev NB, Erbe A, Bao Z, *Phys Rev Lett* **92**:186805/1–186805/4, 2004.
6. Gelinck GH, van Veenendaal E, Coehoorn R, *App Phys Lett* **87**:073508/1–073508/3, 2005.
7. Halls JJM, Walsh CA, Greenham NC, Marseglia EA, Friend RH, Moratti SC, Holmes AB, *Nature* **376**:498–500, 1995.
8. Wang X, Perzon E, Delgado L, De la Cruz P, Zhang F, Langa F, Andersson MR, Inganas O, *Appl Phys Lett* **85**:5081–5083, 2004.
9. Senevirathna MKI, Pitigala PKDDP, Tennakone K, *Phys Chem B* **109**:16030–16033, 2005.
10. Braun D, Heeger AJ, *Appl Phys Lett* **58**:1982–1984, 1991.
11. Ohmori Y, Uchida M, Muro K, Yoshino K, *Jpn J Appl Phys* **30**:L1941–L1943, 1991.
12. Grem G, Leditzky G, Ullrich B, Leising G, *Adv Mater* **4**:36–37, 1992.
13. Grem G, Leditzky G, Ullrich B, Leising G, *Synth Met* **51**:383–389, 1992.
14. Ranger M, Rondeau D, Leclerc M, *Macromolecules* **30**:7686–7691, 1997.
15. Grice AW, Bradley DDC, Bernius MT, Inbasekaran M, Wu WW, Woo EP, *Appl Phys Lett* **73**:629–631, 1998.
16. Gill RE, Malliaras GG, Wildeman J, Hadziioannou G, *Adv Mater* **6**:132–135, 1994.
17. Berggren M, Inganas O, Gustafsson G, Rasmusson J, Andersson MR, Hjertberg T, Wennerstrom O, *Nature* **372**:444–446, 1994.
18. Andersson MR, Berggren M, Inganas O, Gustafsson G, Gustafsson-Carlberg JC, Selse D, Hjertberg T, Wennerstrom O, *Macromolecules* **28**:7525–7529, 1995.
19. Suramitr S, Kerdcharoen T, Srikhirin T, Hannongbua S, *Synth Met* **155**:27–34, 2005.
20. Poolmee P, Hannongbua S, *J Theor Comput Chem* **3**:481–489, 2004.
21. Poolmee P, Ehara M, Hannongbua S, Nakatsuji H, *Polymer* **46**:6474–6481, 2005.
22. Salzner U, *J Phys Chem A* **107**:119–134, 2003.

23. Karpfen A, Choi CH, Kertesz M, *J Phys Chem A* **101**:7426–7433, 1997.
24. Burns DM, Iball J, *Proc Roy Soc (London) A* **227**:200–214, 1955.
25. Bongini A, Bottoni A, *J Phys Chem A* **103**:6800–6804, 1999.
26. Burrows PE, Shen Z, Bulovic V, McCarty DM, Forrest SR, Cronin JA, Thompson ME, *J Appl Phys* **79**:7991–8006, 1996.
27. Zeng G, Yu WL, Chua SJ, Huang W, *Macromolecules* **35**:6907–6914, 2002.
28. Liao LS, Fung MK, Lee CS, Lee ST, Inbasekaran M, Woo EP, Wn WW, *Appl Phys Lett* **76**:3582–3584, 2000.